

Abundance of NH₃ on Jupiter Inferred from Microwave Radiometry Data

ROBERT J. RICHARDSON*

Martin Marietta Aerospace, Denver, Colo.

Measurements of the thermal disk temperature of Jupiter have been made at several microwave frequencies. Disk temperatures are of interest at these long wavelengths because they penetrate into the atmosphere below the clouds, providing some data on the composition and structure of the atmosphere in this region. NH₃ abundance in a number of possible models of the Jupiter atmosphere were determined by computing disk temperature vs frequency curves for each model with varying NH₃ abundance and comparing these results with the measured disk temperatures. Microwave absorption losses were also calculated for these model atmospheres.

Nomenclature

$a_{\text{NH}_3}, a_{\text{H}_2}, a_{\text{He}}$	= experimentally determined coefficients for NH ₃ line broadening
$A_{\text{NH}_3}, A_{\text{H}_2\text{O}}, A_{\text{H}_2}, A_{\text{He}}$	= abundances or ratio by volume in the model atmosphere of the gases indicated by the subscripts
$b_{\text{NH}_3}, b_{\text{H}_2}, b_{\text{He}}$	= experimentally determined coefficients for NH ₃ line broadening
f	= frequency, GHz
f_c	= Debye cutoff frequency for H ₂ O, GHz
H	= altitude in the model atmosphere, km, measured from the 1 atm pressure level
$\text{Im}(x)$	= imaginary part of x
M	= cloud density, g/m ³
P	= total pressure, atmospheres
$P_{\text{NH}_3}, P_{\text{H}_2\text{O}}, P_{\text{H}_2}, P_{\text{He}}$	= partial pressures of the gases indicated in the subscripts, atmospheres
P_{SAT}	= saturation pressure of NH ₃
r	= normalized disk radius
S_B	= shape factor in the Ben-Reuven formulation of gaseous absorption due to molecular resonances
S_V	= shape factor in the Van-Vleck formulation of gaseous absorption due to molecular resonances
T	= temperature, degrees Kelvin
T_{SAT}	= saturation temperature of NH ₃
Z	= integration variable taken along a raypath
$\alpha_{\text{NH}_3}, \alpha_{\text{H}_2\text{O}}, \alpha_c$	= absorption coefficients, optical depths per km, due to gaseous NH ₃ , gaseous H ₂ O, and droplet clouds, respectively
γ	= linewidth parameter used in the Ben-Reuven shape factor, GHz
$\epsilon_j, \epsilon_r, \epsilon_i, \epsilon_\infty, \epsilon_0$	= relative dielectric constants for H ₂ O
ζ	= linewidth parameter used in the Ben-Reuven shape factor, GHz
μ	= microns wavelength
$\Delta\nu$	= H ₂ O absorption linewidth, GHz
ν_0	= center frequency of the NH ₃ inversion spectrum, 23.4 GHz
σ	= electrical conductivity, mhos cm ⁻¹

Introduction

RADIATION emanating from Jupiter at wavelengths greater than about 3 cm has a significant nonthermal component which masks the thermal radiation. However, there have been several measurements made at these long

Table 1 Jupiter disk temperatures

Reference	Frequency, GHz	Temperature Deg. K
1	5.00	224 ± 15
2	2.88	260 ± 35
3	1.43	450 ± 75

wavelengths that allow an approximate separation of the thermal and nonthermal components of the radiation through the use of polarization and interferometric data.¹⁻³ These results are tabulated below in Table 1 and are also shown in Fig. 2-5.

Thermal disk temperatures at these long wavelengths are of interest because they penetrate into the atmosphere below the clouds, providing some data on the composition and structure of the atmosphere in this region. This paper describes how these Earth-based radiometry data were used to determine NH₃ abundance in a number of possible models of the Jupiter atmosphere.

Disk temperatures in the microwave frequencies for any of the giant outer planets are determined wholly by the atmosphere. Effects due to the planet surface are completely obscured by the very thick and lossy atmosphere. Given a model atmosphere, i.e., a postulated profile of pressure and temperature vs altitude together with an assumed set of abundances of the principal constituents, the resulting thermal disk temperature can be computed as a function of frequency or wavelength. The computations are summarized in subsequent sections of this paper. This curve can then be compared to the observed data given in Table 1. The disk temperature vs frequency characteristic is a sensitive function of the assumed abundance of the principal absorber, gaseous NH₃. The technique used to select the most likely NH₃ abundance for a given model atmosphere was simply to vary this abundance until a good match with the data in Table 1 was realized.

Computation of Absorption Coefficients

The first step in the computation of disk temperatures is the computation of the absorption coefficient α , a function of elevation in the model atmosphere. As stated above, the principal source of microwave absorption is gaseous NH₃. Other sources of absorption are gaseous H₂O and clouds.

The method of computing absorption coefficients for gaseous NH₃ is taken from DeWolf.⁴ He uses the Ben-Reuven expression

$$\alpha_{\text{NH}_3}(f) = \frac{1.98 \times 10^6 P_{\text{NH}_3} f^2}{T^2} S_B \quad (1a)$$

Presented as Paper 73-128 at the AIAA 11th Aerospace Sciences Meeting, Washington, D. C., January 10-12, 1973; submitted January 4, 1973; revision received May 21, 1973.

Index categories: Atmospheric, Space, and Oceanographic Sciences; Spacecraft Communication Systems.

*Head, RF Systems Unit, Electronics R and D.

where S_B is the Ben-Reuven shape factor

$$S_B = \frac{2(\gamma - \zeta)f^2 + 2(\gamma + \zeta)(\nu_0^2 + \gamma^2 - \zeta^2)}{[\nu_0^2 - f^2 + \gamma^2 - \zeta^2]^2 + 4f^2\zeta^2} \quad (1b)$$

and where

$$\begin{aligned} \gamma &= a_{\text{NH}_3} P_{\text{NH}_3} + a_{\text{H}_2} P_{\text{H}_2} + a_{\text{He}} P_{\text{He}} \\ \zeta &= b_{\text{NH}_3} P_{\text{NH}_3} + b_{\text{H}_2} P_{\text{H}_2} + b_{\text{He}} P_{\text{He}} \end{aligned} \quad (2)$$

The experimentally determined coefficients are:

$$\begin{aligned} a_{\text{NH}_3} &= 16.3(300/T) \\ b_{\text{NH}_3} &= 10.7(300/T) \\ a_{\text{H}_2} &= 1.9(300/T)^{-6} \\ b_{\text{H}_2} &= 1.1(300/T)^{-6} \\ a_{\text{He}} &= 0.61(300/T)^{-7} \\ b_{\text{He}} &= 0.30(300/T)^{-7} \end{aligned} \quad (3)$$

Expressions for absorption coefficients due to gaseous H_2O were taken from Bean⁵ for low pressures and Ho⁶ for high pressures, both modified for H_2 -He foreign gases. Bean's expression (after modification) is

$$\alpha_{\text{H}_2\text{O}}(f) = \alpha_1 + \alpha_2 \quad (4)$$

The nonresonant term is

$$\alpha_1 = 27.4 \frac{P_{\text{H}_2\text{O}}}{T^2} \Delta\nu f^2 \quad (5)$$

The resonant term corresponding to the absorption line at 22.2 GHz is

$$\alpha_2 = 5.896(P_{\text{H}_2\text{O}}/T)f^2(293/T)^{5/2} \exp(-6.44/T)S_V \quad (6)$$

where S_V is the Van-Vleck shape factor

$$S_V = \frac{\Delta\nu}{(f - 22.2)^2 + f^2} + \frac{\Delta\nu}{(f + 22.2)^2 + f^2} \quad (7)$$

The linewidth $\Delta\nu$ is given by

$$\Delta\nu = (2.02P_{\text{H}_2} + 1.72P_{\text{He}})(318/T)^{1/2} \quad (8)$$

The Ho expression is

$$\alpha_3 = \frac{1.7 \times 10^8 f^2 P_{\text{H}_2\text{O}}(10.23P_{\text{H}_2} + 8.3P_{\text{He}})}{T^5} \quad (9)$$

Since Ho's expression does not include a resonant term for the 22.2 GHz line, which will be resolved at lower pressures, α_2 was also added to Ho's expression. The question of where to change from the Bean to the Ho approach was resolved by taking

$$\alpha_{\text{H}_2\text{O}} = \text{least of } (\alpha_1 + \alpha_2, \alpha_2 + \alpha_3) \quad (10)$$

The only clouds that give significant absorption are the liquid droplet water-ammonia solution clouds. These are not present in all atmosphere models. The method used to determine the presence, thickness, density, and composition of these clouds is discussed in a subsequent section of this paper. Calculation of these losses is complicated by the electrical conductivity of the solution, a function of solution strength, which varies with elevation within the cloud. In order to determine the effect of these clouds, it is necessary to determine the dielectric constant and electrical conductivity of the solution as a function of temperature and solution strength. Conductivity α as a function of solution strength and temperature, is taken from Condon and Osdshaw.⁷ The complex dielectric constant

$$\epsilon_j = \epsilon_r + i\epsilon_i \quad (11)$$

is computed using the Debye formulas,⁸

$$\epsilon_r = \frac{(\epsilon_\infty + \epsilon_0)(f/f_c)^2}{1 + (f/f_c)^2} \quad (12a)$$

$$\epsilon_i = \frac{(\epsilon_\infty - \epsilon_0)(f/f_c)^2}{1 + (f/f_c)^2} + \frac{1800\sigma}{f} \quad (12b)$$

ϵ_∞ , ϵ_0 , and f_c are tabulated in Welch and Rea⁸ as functions of temperature. ϵ_j is then used in

$$\alpha_c = 0.06283 M \cdot f \cdot \text{Im}[-(\epsilon_j - 1)/(\epsilon_j + 2)] \quad (13)$$

from Bean.⁵

All of these absorption coefficients are then added to give $\alpha(f, H)$. It can be seen from Eqs. (1-10) that gaseous absorption due to either NH_3 or H_2O scales approximately as f^2 over the frequency band of interest in this paper, which is low relative to the absorption line frequencies. This is not true of cloud absorption loss. The contribution due to the first term in Eq. (12b) does go approximately as f^2 . However, the contribution due to the second (conductivity-related) term is essentially independent of frequency over the band of interest. It was found in all cases that this contribution was quite small, and the $\alpha(f, H)$ scaled nearly as f^2 over the band of interest.

Model Atmospheres

It is not the intent of this paper to detail the procedures used by various investigators in the construction of model atmospheres for Jupiter. This is presented in a number of papers, including Refs. 9-12 and in references cited in these papers. A brief outline of one approach is given below. Generally, given a range of uncertainties in the observed data, the procedure has been to construct several models which span these uncertainties (e.g., a "warm," a "nominal" and a "cool" model) rather than a single model.

There is general agreement from astronomical and radiometric observations that the elemental composition of the atmosphere of Jupiter is similar to that of the sun, consisting primarily of H_2 and He, with small amounts of other gases. Mean molecular weight (g/mole) is estimated to range between 2.14 and 2.7, with the former giving a hydrogen-rich and the latter a helium-rich model. The atmosphere is assumed to be at adiabatic-hydrostatic equilibrium. This assumption, together with values assumed for gravitational acceleration and mean molecular weight, fixes the temperature lapse rate. It forces the helium-rich models to be warm relative to the hydrogen-rich models, i.e., they will have a larger temperature lapse rate.

Fixing the pressure corresponding to one specific temperature will then permit construction of the complete pressure-temperature profile of the troposphere. This can be inferred from radiometry measurements near 120μ where H_2 is the dominant absorber. These data give a correspondence between a temperature of 125°K and a partial pressure of $\frac{1}{4}$ atmosphere of H_2 .

Radiometry data in the IR region can be used to estimate the abundance of CH_4 relative to that of H_2 . Lewis⁹ infers the abundance of NH_3 and H_2O from this result by assuming that the C:N:O abundance ratios are the same as those on the sun and that these elements are wholly converted to CH_4 , NH_3 , and H_2O on Jupiter. (The O abundance is modified by the assumption that various metallic oxides are also formed.) This gives an NH_3 abundance, A_{NH_3} , that ranges from 0.0011 to 0.0019 over his models. The authors of Ref. 10 use the same technique but different radiometry data, giving a much lower A_{NH_3} , ranging from 0.00007 to 0.00035 over their models. Cook,¹¹ in a paper that is a companion to this paper, uses a different technique. He retains the modified N:O solar abundance ratio to fix the relative abundances of NH_3 and H_2O , but he determines A_{NH_3} using the technique described in this paper. As described below, this gives an A_{NH_3} that ranges from 0.00017 to 0.0017 over his models.

It is clear from the aforementioned results that there remains a considerable uncertainty in the value of A_{NH_3} on

Jupiter. However, it is encouraging that there is good correspondence between the maximum value for A_{NH_3} predicted separately by Lewis and Cook using two distinctly different approaches. If one assumes an $A_{\text{H}_2\text{O}}$ of around 0.25 (which is near the helium-rich limit of likely atmosphere compositions), there is very good agreement in the A_{NH_3} given by the Lewis and the Cook approaches, with both giving a value in the vicinity of 0.0016.

Cloud and Saturation Models

All of the atmosphere models cited above have an NH₃ ice cloud as the top or visible cloud layer. This is the only cloud that would occur in very dry models with low NH₃ and H₂O abundances. As the abundances of these cloud-forming compounds are increased, other clouds will appear below the visible cloud, including various combinations of NH₃ and H₂O ices. Finally, if A_{NH_3} and $A_{\text{H}_2\text{O}}$ are sufficiently large, the liquid droplet NH₃-H₂O solution cloud will appear as the lowest cloud layer. The method used by Cook¹¹ to compute the composition, density, state, elevation, and thickness of these cloud layers was taken from Lewis.⁹

The abundance of gaseous NH₃ was set as the value A_{NH_3} specified by the model for elevations below the saturation level. Above this level it was determined from

$$A'_{\text{NH}_3} = \frac{A_{\text{NH}_3} \cdot T_{\text{SAT}} \cdot P_{\text{SAT}}}{T \cdot P \exp[25.88(T_{\text{SAT}}/T - 1)]} \quad (14)$$

where T_{SAT} , P_{SAT} are the temperature and pressure at the saturation level and T , P are the temperature and pressure at the elevation corresponding at A'_{NH_3} (from Hogan¹²). A similar expression was used for the abundance of gaseous H₂O. Partial pressures were computed from

$$P_x = A_x/P \quad (15)$$

As described earlier, A_{NH_3} and $A_{\text{H}_2\text{O}}$ were varied in each model atmosphere considered (with the $A_{\text{NH}_3}:A_{\text{H}_2\text{O}}$ ratio held constant) until a value of A_{NH_3} giving a good match with the data in Table 1 was found. This required the computation of a new cloud profile for each assumed value of A_{NH_3} .

Computation of Disk Temperatures

The temperature seen looking along any raypath into a deep atmosphere from above is given by¹³

$$T_R = \int_{Z_0}^{\infty} \alpha(Z) T(Z) \exp \left[- \int_{Z_0}^Z \alpha(x) dx \right] dZ \quad (16)$$

where Z_0 is at the top of the atmosphere and the integration is taken downward along the raypath. This integration can be truncated at a depth giving a total absorption of around 3 optical depths. The atmosphere below this point contributes little to the observed temperature since its upward-directed radiation is largely absorbed in the atmosphere above it. This means that the infinite upper limit in integral (16) can be replaced by any Z greater than that giving

$$\int_{Z_0}^Z \alpha(X) dx = 3$$

with little change in T_R . The disk temperature seen by an observer on Earth is computed by averaging T_R across the disk. The geometry is sketched in Fig. 1, which shows a cross section of the planet and two rays, one emitted at the sub Earth point and one emitted near the planet limb. The angle between the raypath and the local vertical increases with dis-

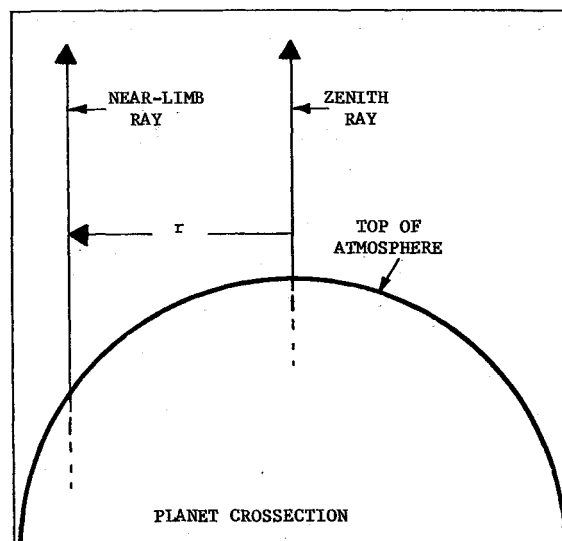


Fig. 1 Typical raypaths, disk temperature computation.

tance from the sub Earth point. This results in a ray temperature that decreases monotonically with distance away from the sub Earth point. The average disk temperature is computed from

$$T_D = 2 \int_0^1 \int_{H_0}^{\infty} \frac{\alpha(H)}{(1-r^2)^{1/2}} \cdot T(H) \cdot \exp \left[- \int_{H_0}^H \frac{\alpha(x) dx}{(1-r^2)^{1/2}} \right] dH dr \quad (17)$$

r is the normalized disk radius ($r = 1$ at the disk edge) used to average Eq. (16) over the area of the disk.

Disk temperature was computed vs f for a number of different atmosphere models, and results were compared with the Earth-based observations given in Table 1. Results for the "nominal" and "cool" models given in Ref. 10 are shown in Fig. 2. Neither of these models give results that match the Earth-based observations very well. The nominal is too warm and the cool is too cool. This was taken as strong evidence that neither of these models were believable in their specified form. However, it was found that either model could be forced to match the Earth-based data by varying the NH₃ abundance

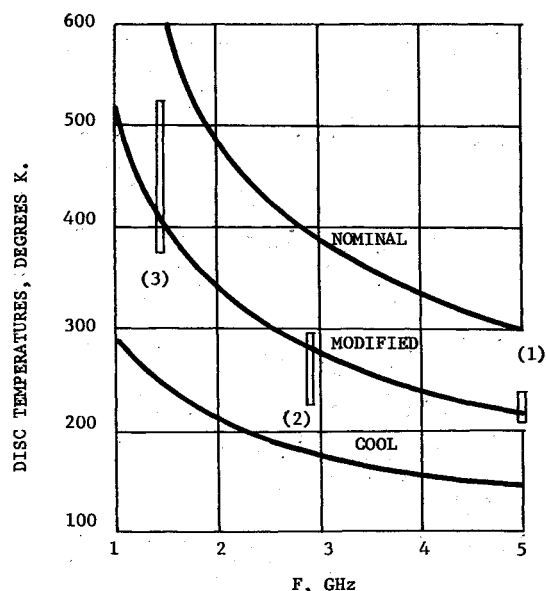


Fig. 2 Disk temperatures, NASA-SP-8069 model atmospheres.

A_{NH_3} until a good fit was achieved. (The ratio of H_2O abundance to NH_3 abundance was held constant.) The required variation in A_{NH_3} was quite large. It was necessary to alter the nominal model from its specified A_{NH_3} value of 0.00015 to the modified value of 0.00059 to give a good match to the Earth-based radiometry data. A_{NH_3} in the cool model was altered from its specified value of 0.00035 to the modified value of 0.00043 to give a good match to the Earth-based radiometry data.

The most interesting feature of these results is that they are strongly affected by the planetary abundance of NH_3 , which is present in the unsaturated atmosphere below the cloud layers. For example, the temperature given in Ref. 3, 450°K, occurs at a pressure of 16 atm in the nominal, 90 km below the lowest cloud. This is in contrast to results given by disk temperature observations at shorter wavelengths (a few centimeters or less) which are determined wholly by the temperature profile in the saturated region above the clouds and therefore cannot be used to infer the planetary abundance of NH_3 .

This technique was then applied to the set of atmosphere models generated by Cook,¹¹ and was used to fix A_{NH_3} in these models. Results are shown in Figs. 3-5. Several curves are plotted to show the sensitivity of the technique to small changes in A_{NH_3} .

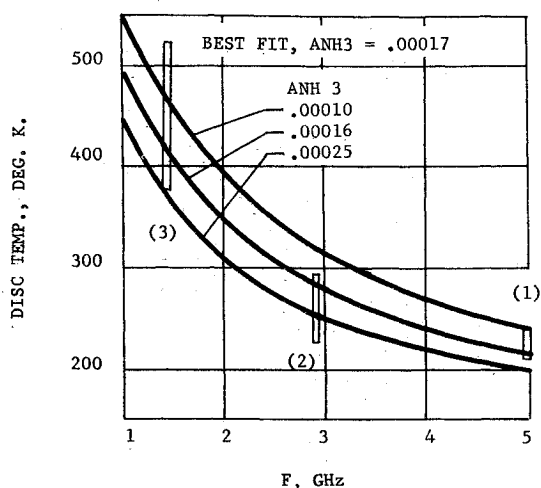


Fig. 3 Disk temperature, Cook "cool" model atmosphere.

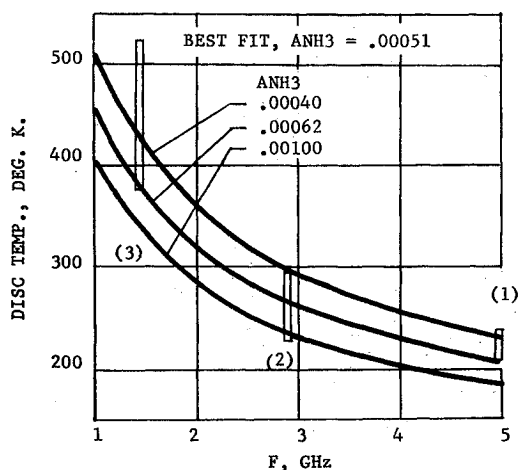


Fig. 4 Disk temperature, Cook "nominal" model atmosphere.

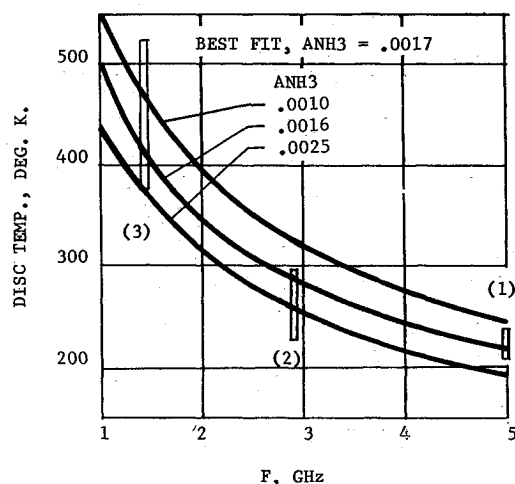


Fig. 5 Disk temperature, Cook "warm" model atmosphere.

Computation of Zenith Absorption

The coefficients given by Eqs. (1-13), converted to dB per km by the factor $10 \log_{10}(e) \cong 4.34$, can be integrated upward from any observation point H to give the zenith absorption in dB seen at that point. Results at $f = 1$ GHz for the five atmosphere models considered in this paper are plotted in Figs. 6 and 7. The zero elevation reference for these plots is the 1 atm pressure level.

Conclusions

The use of Earth-based uhf radiometry data has been shown to be a valuable tool for estimating the planetary abundance of NH_3 on Jupiter, given an atmosphere model that is well-defined in other respects. The technique is quite sensitive to variations in the assumed pressure-temperature profile of the atmosphere. Given present uncertainties in this profile, an accurate determination of NH_3 abundance cannot be made at this time. A warm, helium-rich model that is near the limit of these uncertainties gives an estimated maximum value for NH_3 abundance of 0.0017. This result agrees well with the value determined by Lewis⁹ using an entirely different approach.

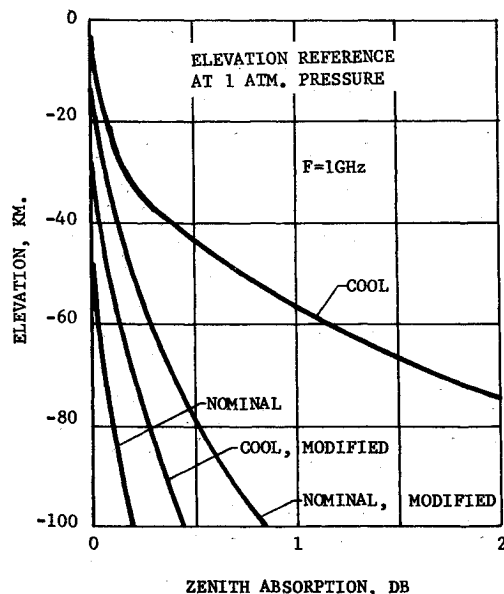


Fig. 6 Zenith absorption loss, NASA-SP-8069 model atmospheres.

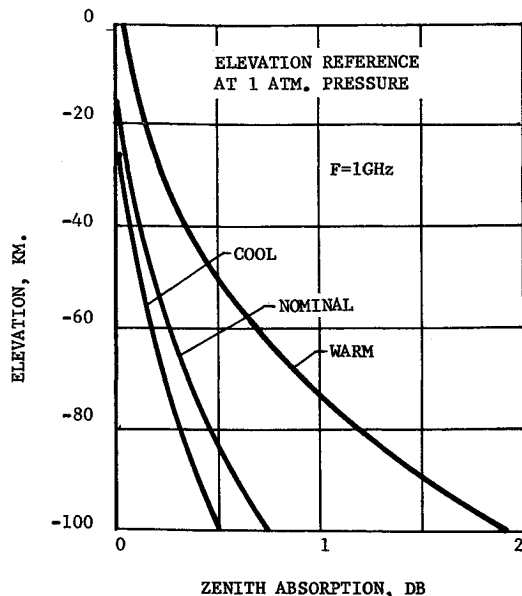


Fig. 7 Zenith absorption loss, Cook model atmospheres.

This technique should be equally effective for any of the large outer planets, all of which are similar in composition, with gaseous NH₃ as the principal absorber of microwave energy. Determination of NH₃ abundance is important for purely scientific reasons. It is also an important factor in the design of planetary entry probes. Atmospheric absorption loss at microwave frequencies has a major impact on the transmitter power requirements for these probes. For this reason, the NH₃ abundance specified in the model atmospheres used

for probe design should be as realistic as possible to avoid overdesign or underdesign of the probe transmitter and energy storage systems.

References

- ¹ Dickel, J. R., "6-cm Observation of Jupiter," *The Astrophysical Journal*, Vol. 148, 1967, p. 535.
- ² Berge, G. L., "An Interferometric Study of Jupiter's Decimeter Radio Emission," *The Astrophysical Journal*, Vol. 146, 1966, p. 767.
- ³ Branson, F. J. B. A., "High Resolution Radio Observations of the Planet Jupiter," *Monthly Notices of the Royal Astronomical Society*, Vol. 139, 1968, p. 155, (data reworked by Berge).
- ⁴ De Wolf, D. A. and Kaplan, G. S., "Investigation of Line-of-Sight Propagation in Dense Atmosphere: Phase III, Part I," Final Rept., Contract NAS2-5310, Nov. 1971, NASA.
- ⁵ Bean, B. R. et al., "Weather Effects on Radar," *Radar Handbook* edited by M. Skolnik, McGraw-Hill, New York, 1970, Chap. 24.
- ⁶ Ho, W. et al., "Laboratory Measurements of Microwave Absorption in Models of the Atmosphere of Venus," *Journal of Geographical Research*, Vol. 71, No. 21, Nov. 1966, pp. 5091-5108.
- ⁷ Condon, E. U. and Odishaw, H., *Handbook of Physics*, McGraw-Hill, New York, 1959, Chap. 9.
- ⁸ Welch, W. J. and Rea, D. G., "Upper Limits of Liquid Water in the Venus Atmosphere," *The Astrophysical Journal*, Vol. 148, No. 6, June 1967, p. L151-L154.
- ⁹ Lewis, J. S., "The Clouds of Jupiter and the NH₃-H₂O and NH₃-H₂S Systems," *Icarus*, Vol. 10, No. 365, 1969.
- ¹⁰ "The Planet Jupiter (1970)," SP-8069, Dec. 1971, NASA.
- ¹¹ Cook, W. S., "Engineering Models for Jupiter's Troposphere and the NH₃-H₂O Cloud System," AIAA Paper 73-129, Washington, D. C., 1973.
- ¹² Hogan, J. S., Rasool, S. I., and Encrenaz, T., "The Thermal Structure of the Jovian Atmosphere," *Journal of the Atmosphere Sciences*, Vol. 26, No. 5, pt. 1, Sept. 1969, p. 898.
- ¹³ King, D. D., "Passive Detection," *Radar Handbook*, edited by M. Skolnik, McGraw-Hill, New York, 1970, Chap. 39.